

Elsevier required licence: © 2021

This manuscript version is made available under the
CC-BY-NC-ND 4.0 license

<http://creativecommons.org/licenses/by-nc-nd/4.0/>

The definitive publisher version is available online at

<https://doi.org/10.1016/j.memsci.2021.119185>

1 **Facile development of comprehensively fouling-resistant and**
2 **self-cleaning high performance aliphatic polyketone-based**
3 **thin film composite forward osmosis membrane for**
4 **treatment of oily wastewater**

5 *Ralph Rolly Gonzales*^{a,b}, *Lei Zhang*^c, *Yuji Sasaki*^b, *Sherub Phuntsho*^a, *Hideto Matsuyama*^{b,c*},
6 *Ho Kyong Shon*^{a,*}

7 ^a Centre for Technology in Water and Wastewater, University of Technology Sydney, New South
8 Wales, Australia

9 ^b Research Center for Membrane and Film Technology, Kobe University, Kobe, Hyogo Japan

10 ^c Department of Chemical Science and Engineering, Kobe University, Kobe, Hyogo, Japan

11 * Corresponding author: Ho Kyong Shon, Email: hokyong.shon-1@uts.edu.au; Hideto
12 Matsuyama, Email: matuyama@kobe-u.ac.jp

13 **Abstract**

14 Forward osmosis (FO) has proven to be a suitable process for treatment of problematic oily
15 wastewater, due to its relatively higher water recovery rate and lower energy requirement, as
16 opposed to pressure-driven membrane processes. Despite the lower membrane fouling propensity
17 during FO operation, the development of comprehensively fouling-resistant and self-cleaning
18 membranes are further desired in FO as a suitable oily wastewater treatment process. In this study,
19 thin film composite (TFC) membranes were developed using reduced aliphatic polyketone (rPK)
20 as the membrane substrate, on which a thin polyamide active layer was formed via interfacial
21 polymerization. Reduction conditions using NaBH_4 were tested, and the suitability of reduction
22 was evaluated in terms of membrane morphology, water wettability, and resistance to oil. The
23 resultant rPK-TFC membrane, whose substrate was reduced with 0.5% (w/w) NaBH_4 for 10 min,
24 exhibited a water flux of $37.8 \text{ L m}^{-2} \text{ h}^{-1}$, when tested in PRO mode. Using a foulant solution
25 containing 1% (v/v) soybean oil, and 100 ppm bovine serum albumin, humic acid, and sodium
26 alginate, the resultant rPK-TFC membrane maintained an outstanding 95% average flux recovery
27 ratio, while the pristine PK-TFC membrane achieved an average flux recovery ratio of 67%. The
28 results indicate that reduction of aliphatic polyketone is a facile method to develop membranes
29 with outstanding water permeability, fouling resistance, and self-cleaning capability.

30

31 **Keywords:**

32 Forward osmosis; Thin film composite membrane; Polyketone; Reduction; Antifouling; Oily
33 wastewater

34 **1. Introduction**

35 Forward osmosis (FO) occurs through the transport of water through a semi-permeable
36 membrane from a stream of lower solute concentration (feed solution, FS) to a stream of higher
37 solute concentration (draw solution, DS). Water transport is mainly governed by the osmotic
38 pressure (π) difference between the FS and the DS. This osmotically-driven membrane process
39 does not require the application of hydraulic pressure, hereby offering the following advantages:
40 sustainable water recovery potential, low fouling tendency, satisfactory contaminant rejection, and
41 less energy consumption depending on chosen application [1]. FO can be applied for a number of
42 applications, which include, but not limited to, desalination [2], resource recovery [3], juice
43 dewatering [4], osmotic power generation [5, 6], and wastewater treatment [7].

44 Due to the wide applicability of FO, it can be a useful process to solve the current water
45 scarcity and increasing demand for clean water, which is primarily caused by the exponential
46 world's population growth and industrialization. Among the various applications of FO,
47 wastewater treatment and reuse are particularly of extreme importance, since not only do these
48 processes augment our usable water supply, issues concerning environmental pollution can also
49 be mitigated [8].

50 Industrialization has brought about the world's dependency in the oil and gas industries, and
51 this has led to the disposal of oil waste into water bodies without any prior treatment. Therefore,
52 oily wastewater, which contains oil, dissolved organic and inorganic substances, and suspended
53 solids, is a huge environmental concern. Not only can oily wastewater negatively affect aquatic
54 life, it can also pose adverse effects on human health and agriculture [7].

55 FO, as mentioned above, is a suitable candidate in mitigation of the environmental impact
56 of oily wastewater; however, the development of robust, highly selective, and fouling-resistant

57 membranes for wastewater treatment-specific osmotic process is highly essential. Several studies
58 have been done on polyamide-based thin film composite (TFC) membranes, which exhibit higher
59 water permeability, higher selectivity, and satisfactory mechanical strength. Thus, in recent,
60 various fabrication methods and membrane modification have been performed to further improve
61 separation performance and fouling resistance. Among these FO membrane modification and
62 fabrication methods include the incorporation of highly porous nano-sized fillers [9, 10],
63 hydrophilic coating [11, 12], electrolyte deposition [13, 14], incorporation of zwitterionic
64 substances [7, 15], and chemical grafting and modification [16, 17].

65 Chemical modification of polyketone is chosen as the approach for membrane development
66 in this study. Ketones are known to be highly reactive compounds, but not as much as aldehydes
67 which share the same carbonyl ($-\text{C}=\text{O}-$) group, primarily due to the presence of the less
68 electrophilic secondary carbon (the carbonyl C atom is surrounded by two hydrocarbon groups).
69 However, the high reactivity of ketone is mainly influenced by the presence of the carbon-oxygen
70 double bond. Ketones are known to produce secondary alcohols after reduction with certain
71 reducing agents such as LiAlH_4 and NaBH_4 .

72 In this study, polyketone was reduced using NaBH_4 prior to interfacial polymerization. The
73 suitability of reduction in preparation of TFC membranes was first determined, and the separation
74 properties and comprehensive fouling resistance against model oil, protein, carbohydrate, and
75 humics foulants were also evaluated. This study aims to provide evidence that a facile chemical
76 modification of the TFC membrane substrate can significantly alter the membrane transport
77 properties and enhance the fouling mitigation and self-cleaning capability during treatment of oily
78 wastewater.

79

80 2. Experimental

81

82 2.1. Chemicals

83 Aliphatic polyketone ($M_w = 200\,000\text{ g mol}^{-1}$) provided by Asahi Kasei Co., Japan was chosen
84 as the polymer for the membrane substrate. The following solvents and chemicals were used for
85 membrane substrate casting: resorcinol (> 99.0 %, Tokyo Chemical Industry Co., Ltd., Japan),
86 methanol (> 99.8 %, Fujifilm Wako Pure Chemical Corporation, Japan), acetone (> 99.8 %,
87 Fujifilm Wako Pure Chemical Corporation, Japan), and hexane (> 99.8 %, Fujifilm Wako Pure
88 Chemical Corporation, Japan). Reduction of the polyketone substrates was performed using
89 sodium borohydrite (sodium tetrahydroborate, NaBH_4 , powder, Fujifilm Wako Pure Chemical
90 Corporation, Japan).

91 During interfacial polymerization, the following substances were used: *m*-phenylenediamine
92 (MPD, Fujifilm Wako Pure Chemical Corporation, Japan), 1,3,5-benzenetricarbonyl trichloride
93 (trimesoyl chloride, TMC, > 98.0 %, Tokyo Chemical Industry Co. Ltd., Japan), (\pm)-10-
94 camphorsulfonic acid (CSA, > 98.0 %, Tokyo Chemical Industry Co. Ltd., Japan), triethylamine
95 (TEA, > 99.0 %, Wako Pure Chemical Industries, Ltd., Japan), sodium dodecyl sulfate (SDS,
96 Fujifilm Wako Pure Chemical Corporation, Japan), and heptane (> 99.3 %, Fujifilm Wako Pure
97 Chemical Corporation, Japan).

98 For fouling resistance studies, the following model foulants were chosen: soybean oil (Wako,
99 Fujifilm Wako Pure Chemical Corporation, Japan), bovine serum albumin (BSA, Wako Pure
100 Chemical Corporation, Japan), humic acid (sodium salt, Sigma-Aldrich, Japan), and sodium
101 alginate (Nacalai Tesque, Inc., Japan).

102 All the substances used in this study were used as received and without further treatment.

103

104 **2.2. Membrane fabrication**

105 **2.2.1. Polyketone substrate casting and subsequent reduction**

106 Polyketone (PK) substrate was prepared by conventional non-solvent-induced phase
107 separation (NIPS) process, according to a previous study [18]. A 10 % (w/w) PK solution was
108 prepared with 65 % (w/w) aqueous resorcinol as solvent. The solution was stirred at 80 °C for 3 h,
109 and degassed at 50 °C overnight. The solution temperature was maintained at 50 °C prior to casting.
110 The solution was poured on a glass plate and was spread using a stainless-steel casting knife with
111 a casting thickness of 400 μm. The nascent PK substrate was afterwards immersed in a 35 % (w/w)
112 aqueous methanol coagulation bath at 25 °C to allow complete phase separation and equipped in
113 steel frames to avoid shrinkage. The substrates were afterwards washed with acetone and hexane
114 successively for 20 min each and air-dried until further use.

115 Reduction of the PK substrate was performed by immersion of the PK membranes in 0.5%
116 (w/w) aqueous NaBH₄ solution for a varied period of time (5 to 30 min), after which, the reduced
117 membranes were washed with acetone and hexane successively for 20 min each, and air-dried until
118 further use.

119

120 **2.2.2. In situ interfacial polymerization and thin film composite membrane preparation**

121 To prepare a PK-based TFC membrane, the selective polyamide layer was formed on one
122 side of the pristine and reduced PK substrates through *in situ* interfacial polymerization described
123 in a previous study [19]. An aqueous amine precursor solution, containing 2.0 % w/w MPD, 1.1 %
124 w/w TEA, 2.3% w/w CSA, and 0.15 % w/w SDS, was first introduced onto one side of the PK
125 substrate for 5 min. The excess solution was afterwards discarded, and the membrane substrate

126 was allowed to stand for 1 min. Air knife was afterwards used to remove the excess amine
127 precursor solution. An organic acyl halide precursor solution, containing 0.15 % w/w TMC in
128 heptane was introduced and made to react with the residual amine precursor for 2 min. The excess
129 acyl halide solution was removed, and the membrane was allowed to stand for 1 min, and
130 afterwards cured at 90 °C for 10 min to complete the reaction. The resultant TFC membrane was
131 washed with copious amounts of deionized (DI) water, stored in DI water, and placed in cool and
132 dark condition prior to testing and characterization.

133

134 ***2.3. Determination of intrinsic transport parameters***

135 Pure water permeability (PWP, A , $L m^{-2} h^{-1} bar^{-1}$) and solute permeability (B , $L m^{-2} h^{-1}$) were
136 determined using a cross-flow reverse osmosis (RO) system with an effective membrane area (A_m)
137 of 8.04 cm^2 , under a pressure of 10 bar, temperature of 25°C, and a flow rate of 150 $mL min^{-1}$
138 ^[20]. DI water and 1000 $mg L^{-1}$ NaCl were used as a feed for determination of A and B , respectively.
139 The equations used for calculation of A and B were reported in a previous study [13].

140

141 ***2.4. Membrane osmotic performance***

142 The osmotic performance of the TFC membranes were evaluated using a custom laboratory-
143 scale FO system [20], with a cell whose effective membrane area is 4.5 cm^2 and two peristaltic
144 pumps (NS Pump NPL-100, Nihon Seimitsu Kagaku Co., Ltd., Japan) delivering the feed and
145 draw solutions, originally 1 L in volume each. FO tests were conducted in two modes: AL-FS (FO
146 mode, active layer facing the feed solution) and AL-DS (PRO mode, active layer facing the draw
147 solution). The hydraulic pressures of both feed and draw were kept at minimum, and the flow rates
148 of the solutions were maintained at $3 \times 10^{-1} L min^{-1}$. The mass of the permeate was measured using

149 an electronic top-loading balance (FX-3000i, A&D Company, Limited, Japan) connected to a
150 computer. Reverse salt flux was evaluated through the change in feed solution conductivity
151 measured by a conductivity meter (LAQUAtwin, Horiba Ltd., Japan). Water flux (J_w) and reverse
152 salt flux (J_s) were calculated using equations presented in previous study [11].

153

154 **2.5. Fouling**

155 1% (v/v) soybean oil-in-water emulsion was first prepared by mixing together soybean oil,
156 water, and 0.01 ppm SDS surfactant, followed by constant stirring for 12 h. Three 1% (v/v)
157 soybean oil-in-water emulsions spiked with 100 ppm of BSA, humic acid, and sodium alginate
158 were also prepared. Individual fouling tests were conducted for 8 h, with the foulant solutions as
159 feed and 1.0 M NaCl as the draw, using the same FO system mentioned above. The concentration
160 of the draw solution was kept constant at 1.0 M by regular addition of NaCl to avoid dilution effect.
161 Total organic carbon analyzer (TOC-VCSH, Shimadzu Co., Japan) was used to measure the oil
162 concentration (C_o) in the DS. C_o , along with the volume of the draw solution (V), at time t is used
163 to calculate oil flux (J_o), as in **Eq. 1**:

$$164 \quad J_o = \frac{C_o V}{A \Delta t} \quad (1)$$

165 A comprehensive fouling solution containing 1% (v/v) soybean oil, 0.05 ppm SDS, and 100
166 ppm each of BSA, humic acid, and sodium alginate was prepared. The membranes were tested for
167 fouling resistance with the comprehensive fouling solution as feed and 1.0 M NaCl as draw for 8
168 h, and then backwashed for cleaning with DI water, and tested for fouling again for another 8 h.
169 The water flux recovered after membrane cleaning, along with the initial water flux, was used to
170 evaluate the flux recovery ratio, which can be calculated as the ratio of the final and the initial
171 water flux values [21].

172

173 **2.6. Membrane characterization**

174 Membrane surface and cross-sectional morphology was characterized using field-emission
175 scanning electron microscopy (FE-SEM, JSF-7500F, JEOL, Japan). The average surface pore size
176 and pore size distribution were determined using SEM image analysis software (Nano Measurer
177 1.2). Measurements were done in triplicate.

178 Surface chemistry was characterized using Fourier transform infrared (FTIR) spectroscope
179 (Nicolet iS5, Thermo Fisher Scientific, Japan) with an attenuated total reflectance detector (ATR;
180 iD5, Thermo Fisher Scientific, Japan) and X-ray photoelectron spectroscopy (XPS, JPS-9010 MC,
181 JEOL, Japan) with Al K α X-rays.

182 The membrane hydrophilicity and oleophobicity were evaluated by an optical contact angle
183 goniometer (Drop Master 300, Kyowa Interface Science Co., Japan) [22]. Water static contact
184 angle measurements were obtained after dispensing a 4 μ L water droplet onto the membrane
185 sample. Underwater oil contact angle was determined using special J-shaped needles which release
186 oil droplets upward. 10–15 μ L oil droplets of soybean oil were contacted with the membrane.

187

188 **3. Results and Discussion**

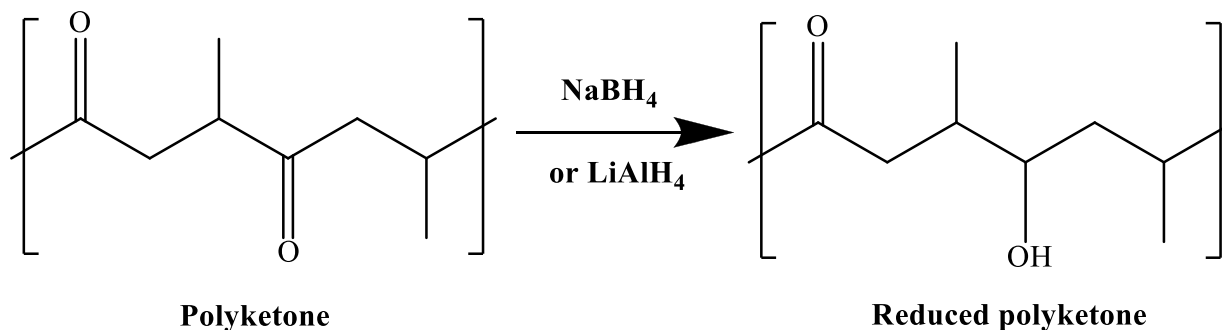
189

190 **3.1. Aliphatic polyketone reduction**

191 Reduction of ketone (R—(C=O)—R') functional groups with common reducing agents,
192 such as LiAlH₄ and NaBH₄ (used in this study), readily forms alcohol functional groups. As shown
193 in **Scheme 1**, reduction of larger chain of ketone functional groups, such as polyketone, results to
194 a partial reduction of the carboxyl groups into alcohol. The hydroxyl (—OH) groups of alcohol

195 readily forms H-bonds with water, thus increasing the overall hydrophilicity and the electrically-
196 neutrality of the polyketone membrane substrate [18].

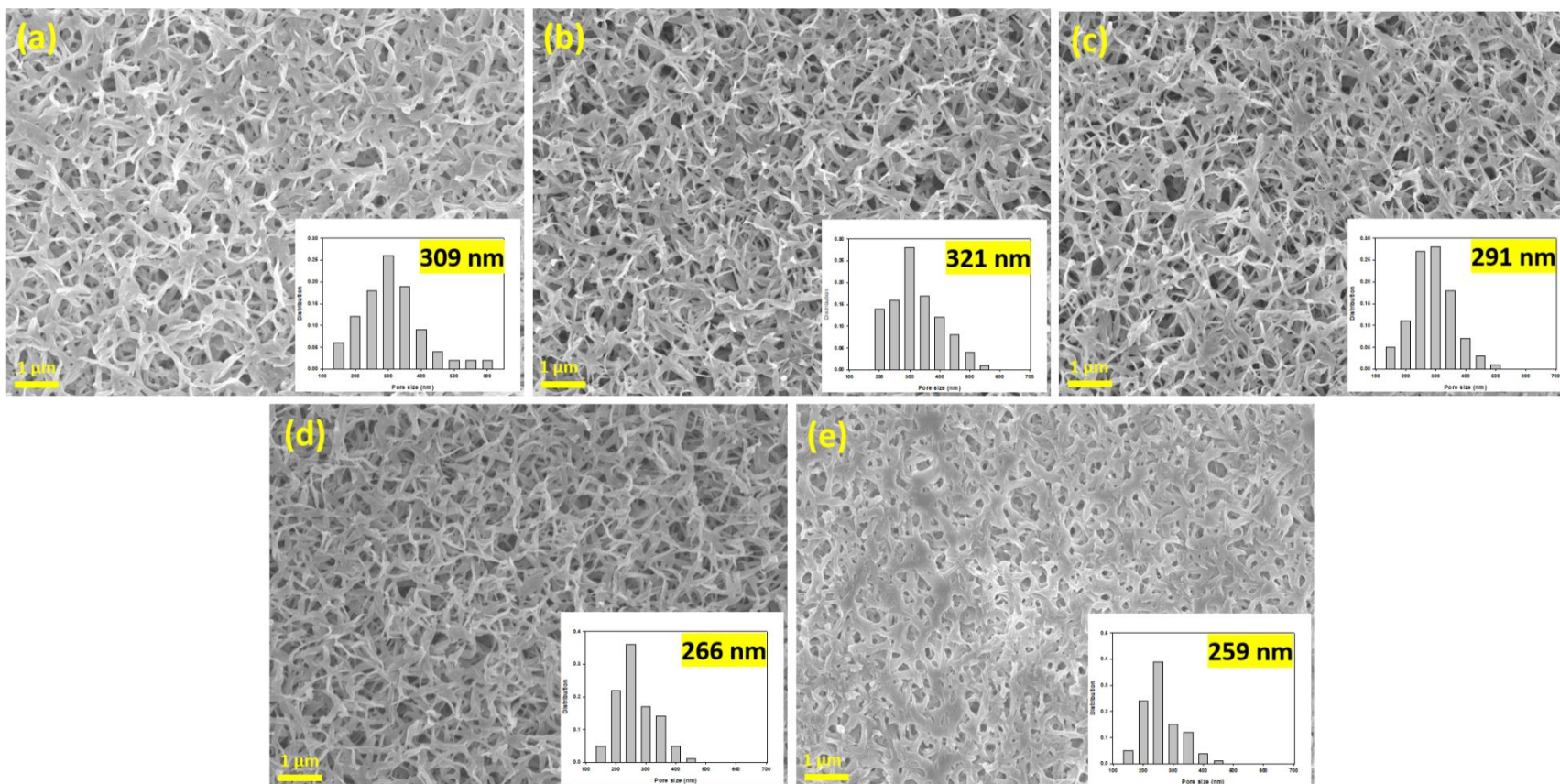
197



199 **Scheme 1.** The reduction of polyketone with NaBH₄ or LiAlH₄ as the reducing agents.

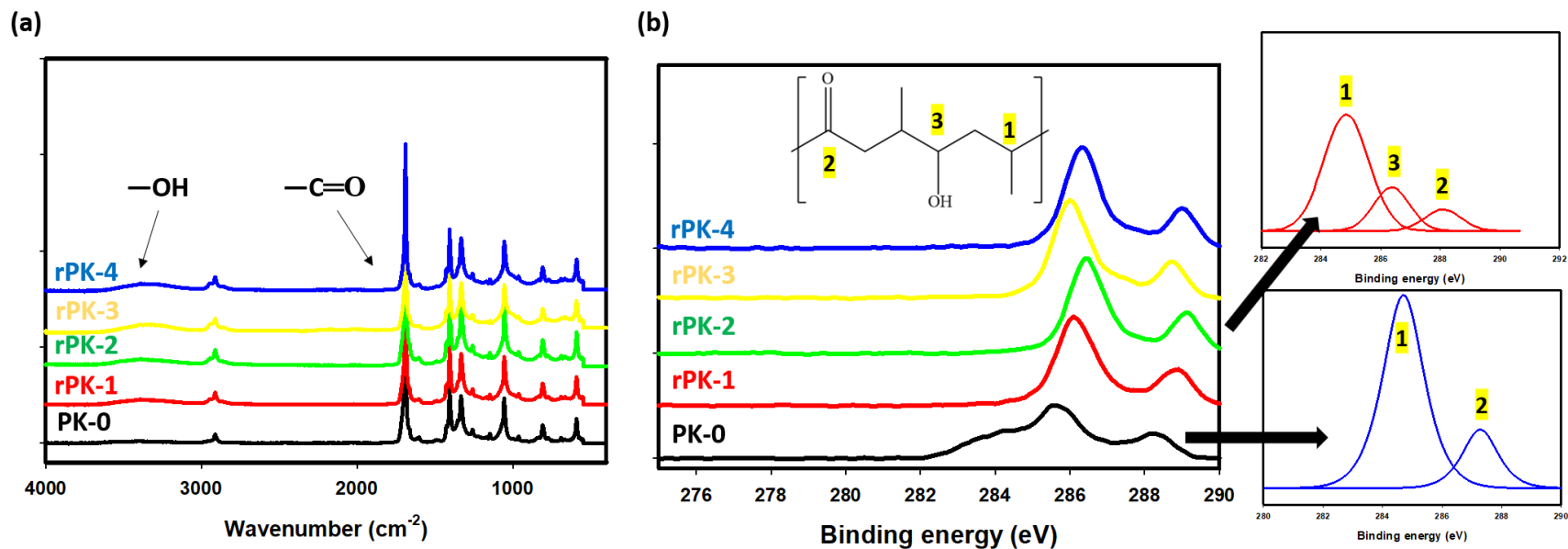
200

201 The morphology of the membranes was characterized using FE-SEM to determine the effect
202 of reduction on the morphology and the formation of defects, if ever. FTIR and XPS were used to
203 determine the success of the reduction of polyketone. The pristine polyketone substrate was first
204 reduced at 0.5% NaBH₄ at different reduction times of 5—30 min. **Figure 1** and **2** show the surface
205 morphology and surface chemistry of the pristine polyketone (PK-0) and the reduced polyketone
206 (rPK-1 to rPK-4, reduced at 5, 10, 20, and 30 min, respectively).



207

208 **Figure 1.** Surface morphology of (a) pristine polyketone (PK-0) and reduced polyketone substrates (rPK-1 to rPK-4) which were reduced
 209 at (b) 5, (c) 10, (d) 20, and (e) 30 min, respectively. Pore size and pore size distribution of the membrane substrates included inset).



210

211 **Figure 2.** Surface chemistry of pristine polyketone (PK-0) and reduced polyketone substrates (rPK-1 to rPK-4) which were reduced at
 212 5, 10, 20, and 30 min, respectively, as shown from the (a) FTIR spectra and (b) XPS C_{1s} spectra of the membrane substrates. The
 213 different carbon species are labeled accordingly: (1) C—C; (2) C=O; and (3) C—OH.

214 The fibrous morphology of polyketone can be seen in all the samples; and the pore size
215 distribution indicates that there was no significant alteration in the pore size of the polyketone
216 substrate during reduction, but a significant marked decrease in pore size was observed with the
217 samples reduced for 20 and 30 min. While rPK-1 and rPK-2 maintained the highly porous structure
218 of pristine polyketone, this was not the case for the rPK-3 and rPK-4, which showed denser skin
219 layers after the chemical modification.

220 The microporous structure of polyketone is interesting to investigate due to its highly
221 symmetric morphology all throughout, with interconnected fibrous structures distributed
222 uniformly all over the substrate. Ease in water permeability and mitigation of water transport
223 resistance are owed to the porous structure of polyketone. What is even more noteworthy is that,
224 unlike other membrane chemical modification processes, polyketone reduction does not
225 significantly alter the membrane's porous structure.

226 Comparing the surface chemistry of the samples, both the FTIR and XPS spectra show that
227 the reduction of the carboxyl groups of the polyketone into alcohol took place. The pristine
228 polyketone substrate showed strong characteristic peaks at around 1050, 1400, and 1690 cm^{-1} ,
229 corresponding to the following respective groups: C—C, —CH₂—, and C=O [23]. The FTIR
230 spectra of the reduced polyketone substrates show a wide stretch at 3400 cm^{-1} , revealing the
231 presence of —OH and indicating the success of the partial polyketone reduction [18]. Until the
232 reduction time of 20 min, the amount of carboxyl groups on the outer surface of the membrane
233 reduced, or hydroxyl groups formed were found to increase as reduction time increases. After
234 reduction for 20 min, the surface chemistry of the reduced polyketone showed similar C_{1s} spectra
235 and speciation. As seen in **Figure 2(b)**, the pristine polyketone substrate also has two species of
236 carbon present, the aliphatic carbon (around 284 eV) and the carbonyl carbon (around 288 eV).

237 After reduction, the rPK substrates exhibit the presence of carbon attached to the hydroxyl group
238 —OH (around 286 eV).

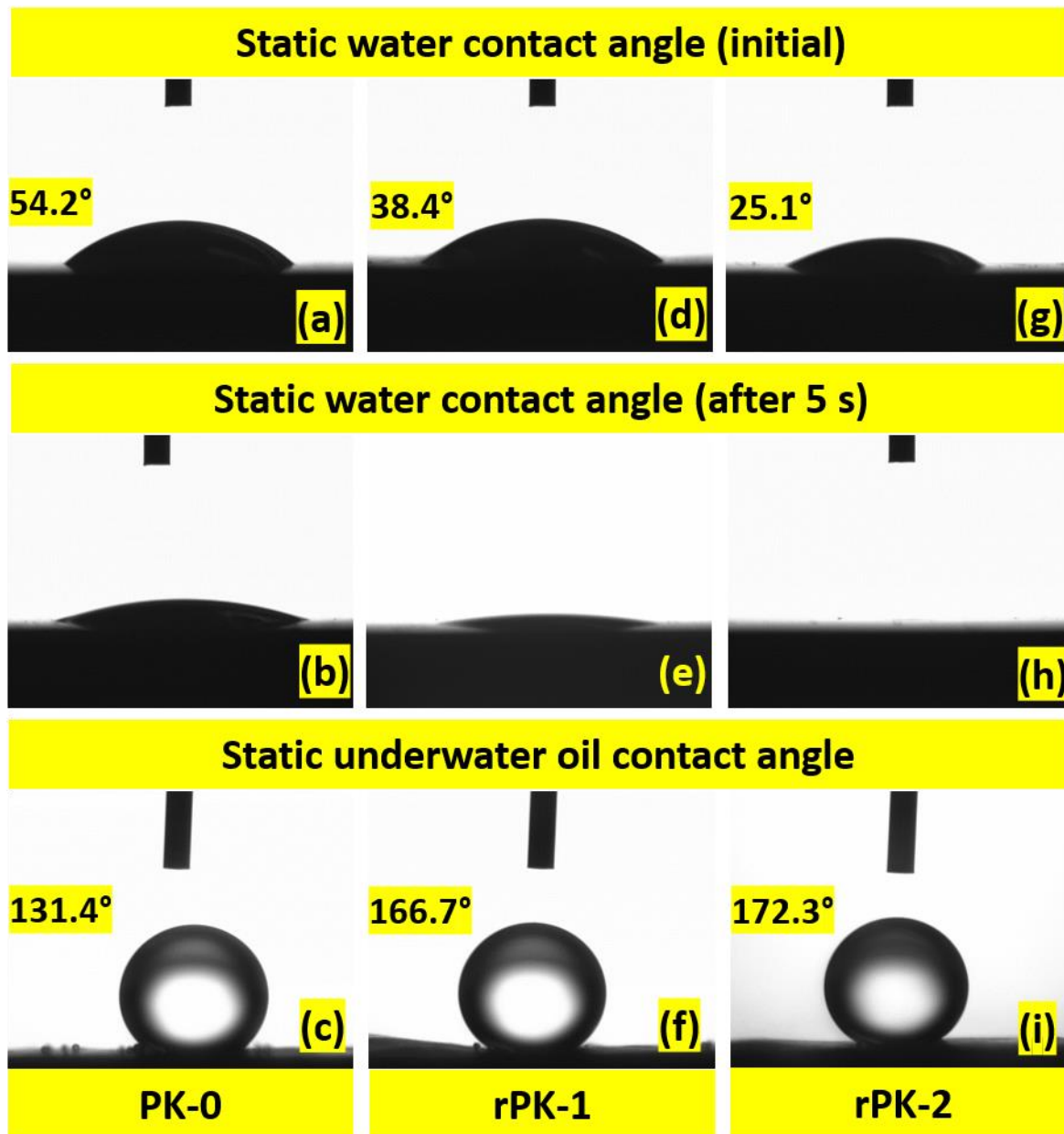
239 The pristine polyketone and reduced polyketone substrates were used for interfacial
240 polymerization to form TFC membranes. The TFC membranes prepared from rPK-3 and rPK-4
241 (reduced for 20 and 30 min, respectively) exhibited polyamide delamination instantaneously as the
242 membranes were placed in DI water right after interfacial polymerization. The delamination of the
243 polyamide active layer can be attributed to a number of factors, particularly, membrane substrate
244 porosity and hydrophilicity. After polyketone reduction at longer periods of 20 and 30 min, there
245 was an observed significant decrease in the substrate surface porosity. It is therefore highly likely
246 that the aqueous amine monomer precursor (MPD) was not able to fully impregnate the reduced
247 membrane substrate due to lower surface porosity. This then results to the formation of polyamide
248 layer with lower cross-linking degree and adhesion with the membrane substrate, and thus, it can
249 easily be removed from the membrane substrate [24]. When exposed in water, the polyamide
250 swells easily, and the polyamide swelling phenomenon undermines its mechanical stability as a
251 result of increased polymer bond distance and weaker chain segments [25]. In relation to the
252 swelling phenomenon, membrane substrate hydrophilicity also plays a huge part in delamination
253 of the polyamide active layer. Deposition of the polyamide active layer on top of the membrane
254 substrate is mainly governed by adhesion forces, and when the membrane substrate is highly
255 hydrophilic, the adhesive forces between the polyamide and the substrate become substantially
256 weaker [26]. The high hydrophilicity of the membrane substrate then allows water to enter the
257 interface of the polyamide and the substrate, resulting in swelling and delamination. For the rest
258 of this study, therefore, only the TFC membranes formed on PK-0, rPK-1, and rPK-2 were
259 considered.

260

261 **3.2. Hydrophilicity and underwater oleophobicity**

262 A particularly important aspect of this study is the influence of the chemical modification of
263 polyketone on the material's hydrophilicity and underwater oleophobicity. These two properties
264 are known to influence the membrane water permeability, and therefore, osmotic performance,
265 and the fouling resistance, as well. **Figure 3** shows the water and underwater oil contact angle
266 profiles of the pristine and reduced polyketone substrates.

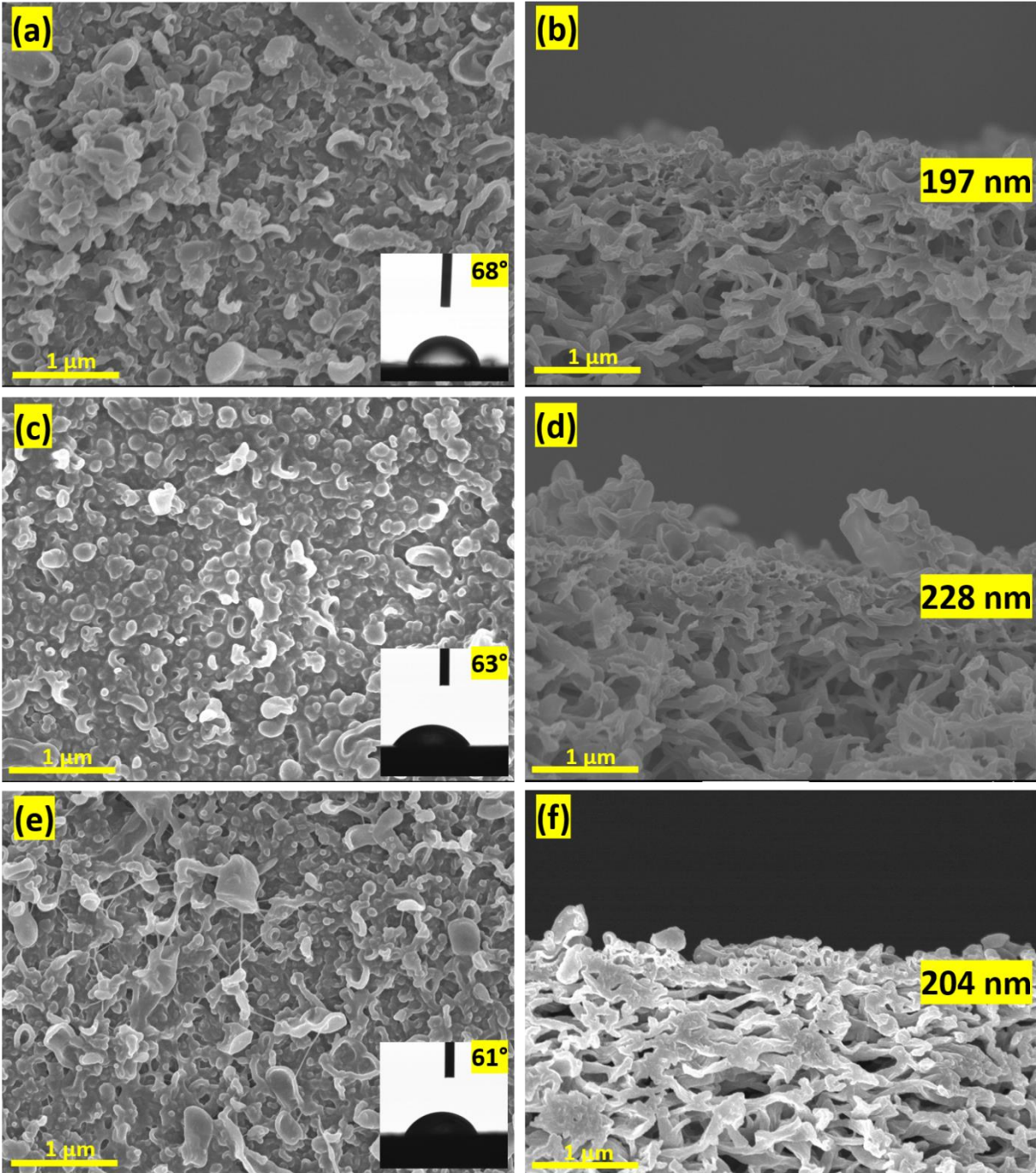
267 Pristine polyketone exhibited a water contact angle of $54.2 \pm 2.8^\circ$. As expected from the
268 chemical modification procedure, the hydrophilicity of the substrates increased after reduction, as
269 evidenced by the significant decrease in the water contact angles. Full penetration of the water
270 droplet into the membrane substrate was achieved after 12 s. rPK-1 showed a water contact angle
271 of $38.4 \pm 1.7^\circ$, while rPK-2 has a water contact angle of $25.1 \pm 2.8^\circ$. For both instances, the water
272 droplet has fully penetrated on the membrane surface in less than 5 s, further indicating the
273 enhanced hydrophilic nature of the reduced polyketone substrate.



274

275 **Figure 3.** Hydrophilicity and underwater oleophobicity of the (a-c) pristine and reduced
 276 polyketone substrates, (d-f) rPK-1 and (g-i) rPK-2, as evidenced by the water contact angle and
 277 underwater oil contact angle. Soybean oil was used as the model oil for the underwater
 278 oleophobicity characterization.

279 The underwater oil contact angle, on the other hand, is a measure of the oleophobicity of the
280 membrane samples, such that a higher underwater contact angle indicates a higher degree of
281 oleophobicity. This particular parameter is influenced by the hydration layer surrounding the
282 membrane, such that, the strength of the hydration layer is directly proportional to the
283 oleophobicity (and oil contact angle). Pristine PK-0 substrate exhibited an underwater oil contact
284 angle of $131.4 \pm 3.9^\circ$, which indicates that polyketone is fairly oleophobic. In the case of rPK-1
285 and rPK-2, both demonstrated outstanding oleophobicity with underwater oil contact angle values
286 of $166.7 \pm 4.8^\circ$ and $172.3 \pm 3.8^\circ$, respectively. It was also noticed that delivering the oil droplets
287 onto the reduced polyketone membrane surface required a higher volume of oil droplet to be
288 allowed to be released by the needle during characterization. It is also worth noting that the oil
289 droplets appeared to be stable on the reduced PK substrate surface even after 5 min. These
290 demonstrate the robust oil-repellant property of the reduced polyketone substrates.



291

292

293

294

Figure 4. Surface and cross-section morphologies of the TFC membranes formed with the [a-b] pristine polyketone substrate (PK-TFC), and reduced polyketone substrates ([c-d] rPK-1-TFC and [e-f] rPK-2-TFC). TFC membrane surface water contact angle are indicated inset.

295 **3.3. TFC membrane morphology**

296 **Figure 4** shows the membrane morphology of the TFC membranes prepared in this study.
297 Characterization of the surface shows the successful formation of the polyamide active layer on
298 the polyketone substrates, regardless of the reduction procedure. The ridge-and-valley structures
299 characteristic of polyamide can be seen, and the cross-section images are used to measure the
300 thickness of the active layer thin films of each membrane sample. The cross-section images show
301 further the interconnected fibril-like structure of polyketone, indicating the high degree of porosity
302 of polyketone. Finger-like porous structures were not visible from the FE-SEM images, while the
303 quite denser sponge-like porous structures were visible towards the bottom surface of the
304 membranes. The surface water contact angles of the three membranes shown in Figure 4 were
305 similar.

306

307 **3.4. Membrane intrinsic transport properties and osmotic performance**

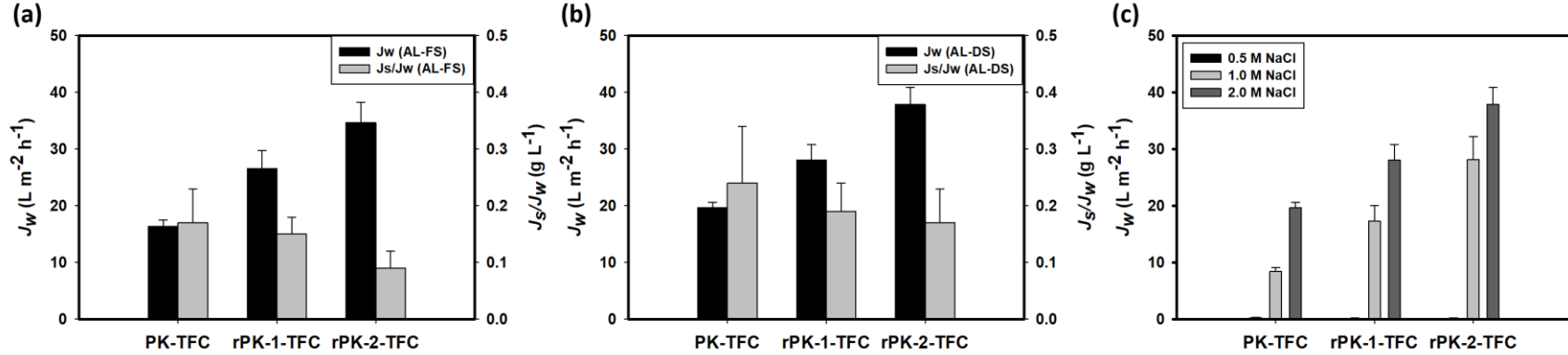
308 The intrinsic membrane transport properties of the TFC membranes are tabulated in **Table**
309 **1**. PK-TFC has an A value of $1.12 \text{ L m}^{-2} \text{ h}^{-1} \text{ bar}^{-1}$, while the most water-permeable membrane rPK-
310 2-TFC has an A value of $1.92 \text{ L m}^{-2} \text{ h}^{-1} \text{ bar}^{-1}$. The formation of a stable polyamide active layer on
311 the substrates was further suggested by the solute rejection capacity of the membranes. All three
312 membranes have outstanding rejection of above 95%, and the solute permeability coefficient (B)
313 were all significantly lower than A , that the B/A value of all three membranes were less than 0.15
314 bar.

315 **Table 1.** The intrinsic transport properties (water permeability coefficient, A , and solute
316 permeability coefficient, B) of the TFC membranes.

Membrane	A ($\text{L m}^{-2} \text{h}^{-1} \text{bar}^{-1}$)	B ($\text{L m}^{-2} \text{h}^{-1}$)	R (%)	B/A (bar)
PK-TFC	1.12 ± 0.13	0.14 ± 0.03	98.0	0.125
rPK-1-TFC	1.45 ± 0.08	0.17 ± 0.05	96.5	0.117
rPK-2-TFC	1.92 ± 0.21	0.28 ± 0.07	95.7	0.146

317

318 Osmotic performance was tested during FO operation of the membranes. Two sets of osmotic
319 performance studies were performed: (1) comparison of the AL-FS and AL-DS orientations using
320 DI water and 1.0 M NaOH as feed and draw, and (2) comparison of the water flux obtained as
321 different concentrations of NaCl were used as the draw. The osmotic performance of the
322 membranes is shown in **Figure 5**. Water flux values obtained at AL-DS orientation are found to
323 be higher than those obtained at AL-FS orientation, since the feed is facing the membrane substrate
324 during AL-DS orientation, thus there is less internal concentration polarization (ICP) [27]. The
325 best performing membrane was rPK-2-TFC, with J_w values of 34.7 and 37.8 $\text{L m}^{-2} \text{h}^{-1}$, for AL-FS
326 and AL-DS orientations, respectively. The J_w of rPK-1-TFC are 26.6 (AL-FS) and 28.0 (AL-DS)
327 $\text{L m}^{-2} \text{h}^{-1}$. These water flux values were significant enhancements from those of the control PK-
328 TFC membrane, whose water flux values for AL-FS and AL-DS orientations are 16.3 and 19.6 L
329 $\text{m}^{-2} \text{h}^{-1}$, respectively. Consistent with the solute permeability coefficient, the TFC membranes also
330 demonstrated outstanding selectivity, with low specific reverse salt flux values. As shown in
331 **Figure 5(c)**, operating FO with different concentrations of draw solution led to higher water flux
332 values as the concentration of draw increased. This is primarily due to the higher osmotic driving
333 force present at higher concentration difference of the draw and feed solutions.



334

335 **Figure 5.** Osmotic performance of the TFC membranes during FO operation: (a-b) the water flux and specific reverse salt flux values
 336 for (a) AL-FS and (b) AL-DS mode with DI water and 1.0 M NaCl as feed and draw, respectively; and (c) the water flux values at AL-
 337 DS mode with DI water as feed and different concentrations of NaCl (0.5 – 2 M) as draw.

338 3.5. Membrane fouling

339 Membrane fouling was observed for the membranes using a variety of representative model
340 foulants. Soybean oil, whose chemical formula is $C_{57}H_{98}O_{12}$, was chosen as the model oil foulant,
341 due to its significantly high molecular weight and capacity to be adsorbed within the pores of the
342 membrane. Representative protein (BSA), carbohydrate (sodium alginate), and humics (humic
343 acid) foulants were also chosen to exhibit the anti-fouling propensity of the membranes. All
344 soybean oil-in-water emulsions used in this study were stabilized using 0.01 ppm SDS surfactant.

345 During the osmotic performance with 1% (v/v) soybean oil-in-water emulsion as feed and
346 1.0 M NaCl as draw, the membranes were tested for FO for 8 h, and the average water flux, specific
347 reverse salt flux, and oil flux values are tabulated in **Table 2**. Despite the presence of oil in the
348 feed, there was no observed significant decrease compared with the water flux values obtained
349 with DI water as feed. After 8 h operation, even the reverse salt flux remained satisfactory and
350 comparable with those of the membranes operated with soybean oil-less feed solution. Oil flux
351 values were also determined to see how effective the membranes are in rejecting oil. PK-TFC
352 exhibited an oil flux value of $0.022 \text{ g m}^{-2} \text{ h}^{-1}$, while the membranes prepared using the reduced
353 polyketone substrate had significantly lower oil flux of 0.010 and $0.006 \text{ g m}^{-2} \text{ h}^{-1}$ for rPK-1-TFC
354 and rPK-2-TFC, respectively, due to the higher substrate hydrophilicity.

355 The antifouling ability of the TFC membranes were put to test during FO operation with
356 model foulants as the feed. Figure 6 shows the water flux profiles of the TFC membranes during
357 FO operation at AL-DS mode for the different model foulants: 1% (v/v) soybean oil-in-water
358 emulsion, and three different solutions of 1% (v/v) soybean oil mixed with 100 ppm each of BSA,
359 sodium alginate, and humic acid. Fouling tests were conducted for a period of 8 h per membrane

360 per foulant solution. The flux values were normalized by division with initial values for better
361 understanding of how the flux was affected during the entire operation.

362 As expected, fouling significantly affected the control PK-TFC membrane. The oil-in-water
363 solution caused a flux decline of 18% after 8 h operation, while the mixture containing humic acid,
364 sodium alginate, and BSA marked flux declines of 26, 37, and 44%, respectively. The foulant
365 molecules entered the substrate porous structure, and the deposition onto the pores caused internal
366 fouling, which resulted to a heightened water transport resistance, thus sharp water flux declines
367 were observed.

368 The rPK-2-TFC membrane exhibited the best antifouling behavior among the three
369 membranes, with rPK-1-TFC not too far behind. Among the four foulant solutions, the soybean
370 oil-in-water emulsion and soybean oil-in-water emulsion mixed with humic acid showed
371 insignificant flux decline over the 8 h operation period, marking only 8 and 11% decrease in water
372 flux for the rPK-2-TFC membrane. With the foulant solutions mixed with sodium alginate and
373 BSA, there were more significant declines in water flux after FO operation of 8 h. 15% water flux
374 declines were observed with the oil-in-water emulsion feed solution spiked with sodium alginate
375 and BSA. Among the three membranes, rPK-1-TFC also showed highly satisfactory fouling
376 mitigation performance, as evidenced by its flux decline of 11, 15, 21, and 23% for the oil-in-water
377 emulsion, as well as the emulsions containing humic acid, sodium alginate, and BSA, respectively.
378 The low water flux decline marked with only oil-in-water emulsion feed solution is due to the
379 oleophobicity of the PK membrane substrate. The same oleophobic nature of the membrane
380 substrate worked as well for rejection of the humics substances, since this type of foulant is known
381 to be consisted of hydrophobic functional groups [28]. In the case of sodium alginate and BSA,
382 these two foulants are characterized by their larger molecular weights, and larger molecules are

383 known to cause more severe fouling. Larger molecules, such as polysaccharides (alginate) and
 384 proteins (BSA), tend to aggregate more on the membrane pores and cause fouling, and can be
 385 mitigated by the presence of negatively-charged surface [29]. Polyketone, when reduced, exhibits
 386 an electroneutral surface [18], which may prove to be useful for oleophobicity, but not for
 387 mitigation of fouling with negative foulants. Thus, even in the case of rPK-2-TFC, 15% water flux
 388 decline was observed when the feed containing sodium alginate and BSA was used.

389 The self-cleaning ability of the membranes was evaluated after a simple backwash in
 390 between the fouling performance tests. The pristine membrane exhibited a flux recovery of 67%
 391 after backwashing. This indicates that while the pristine PK membrane is generally hydrophilic
 392 and oleophobic, the oil and foulants adsorbed on the membranes are not easily washed out. In the
 393 case of the membranes with reduced polyketone substrates, flux recovery was observed to be as
 394 high as 89% and 95% for rPK-1-TFC and rPK-2-TFC, respectively. The self-cleaning ability
 395 during wetting with water is among the known properties of highly hydrophilic membranes. The
 396 added oleophobic characteristic of the reduced polyketone substrates further aids in the self-
 397 cleaning process, as water can be adsorbed onto the pores despite being fully wetted by oil. These
 398 results indicate that antifouling and self-cleaning membranes can be used for effective treatment
 399 of problematic feed water, such as oily wastewater.

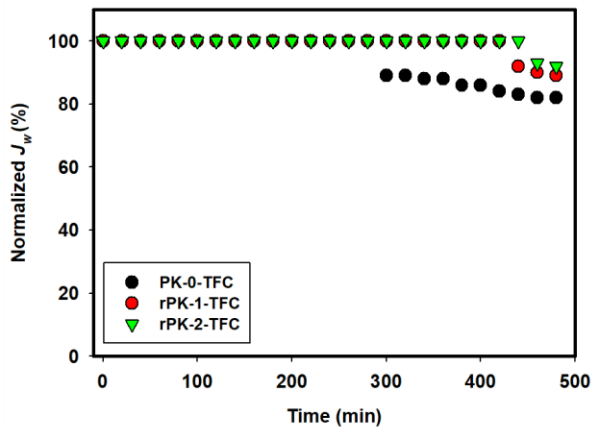
400

401 **Table 2.** Osmotic performance of the TFC membranes during FO operation using 1.0 M NaCl and
 402 1 (v/v) soybean oil-in-water emulsion as the draw and feed, respectively.

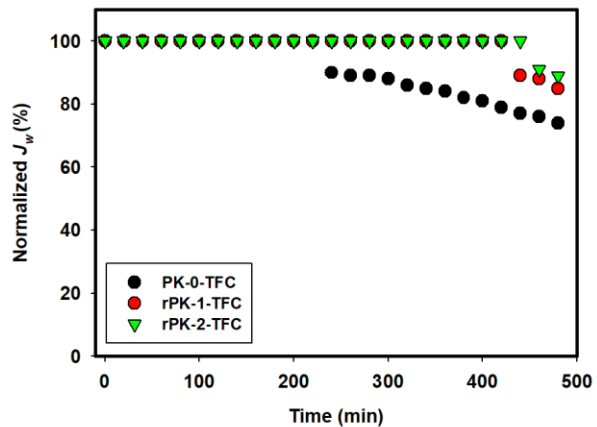
Membrane	Water flux, J_w ($\text{L m}^{-2} \text{h}^{-1}$)	Specific reverse salt flux, J_s/J_w (g L^{-1})	Oil flux, J_o ($\text{g m}^{-2} \text{h}^{-1}$)
PK-TFC	13.8 ± 1.27	0.36	0.022
rPK-1-TFC	25.8 ± 2.11	0.29	0.010
rPK-2-TFC	34.9 ± 2.86	0.32	0.006

403

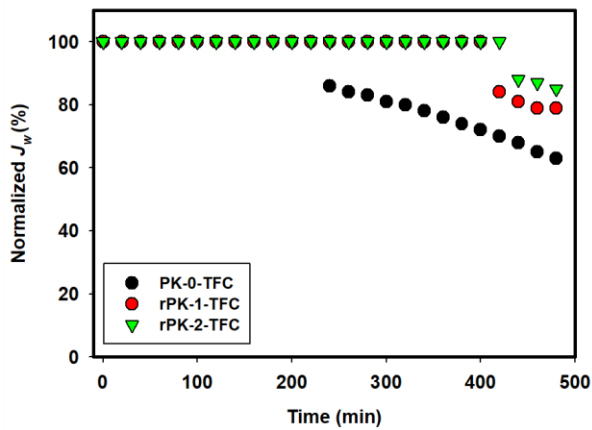
(a) Feed: 1% (v/v) soybean oil



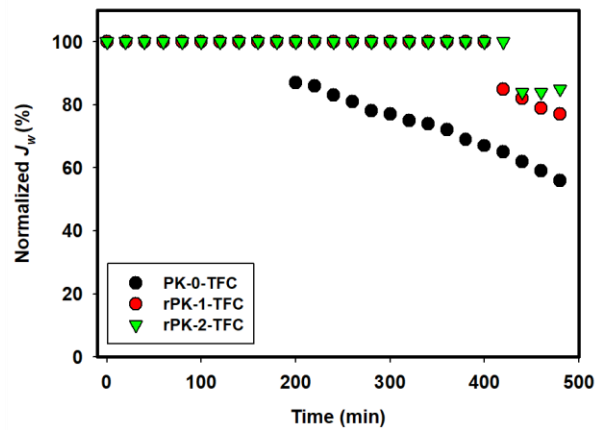
(b) Feed: 1% (v/v) soybean oil + 100 ppm humic acid



(c) Feed: 1% (v/v) soybean oil + 100 ppm sodium alginate

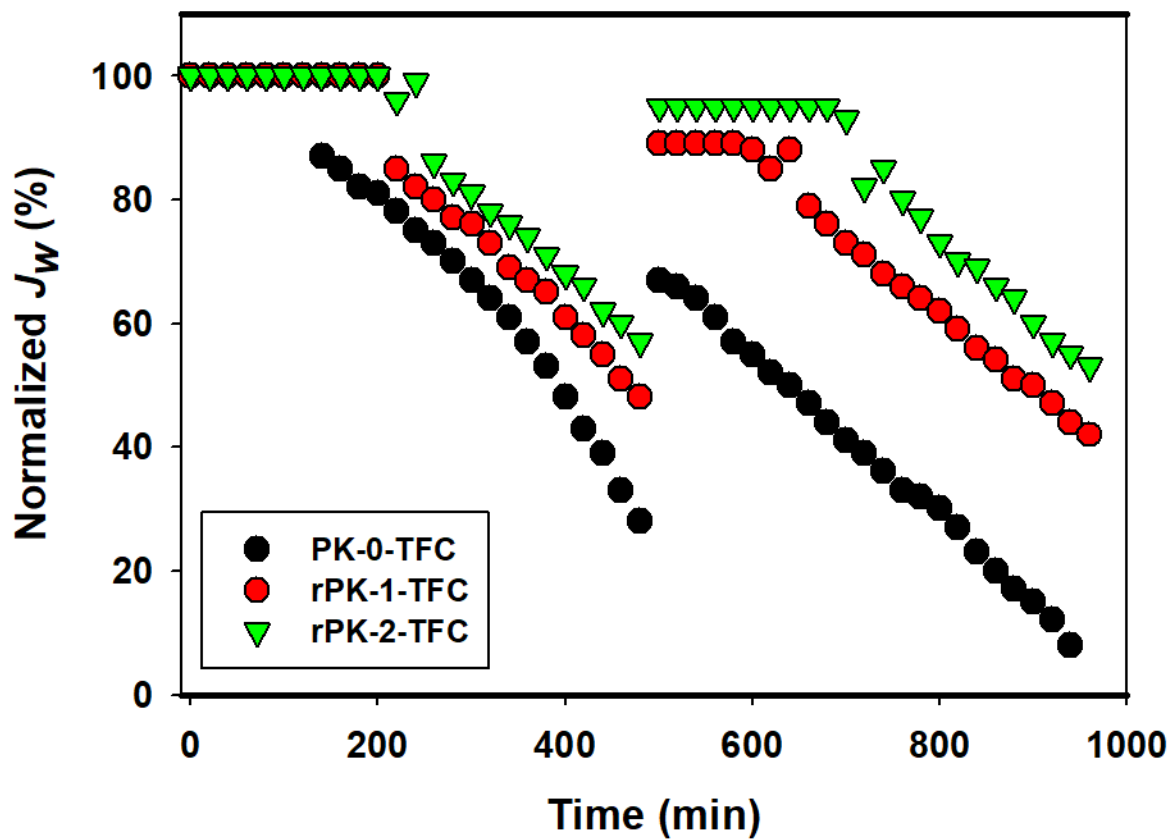


(d) Feed: 1% (v/v) soybean oil + 100 ppm BSA



404

405 **Figure 6.** Water flux profiles of the TFC membranes during FO operation at AL-DS mode for the
406 different model foulants: (a) 1% (v/v) soybean oil; (b) 1% (v/v) soybean oil and 100 ppm humic
407 acid; (c) 1% (v/v) soybean oil and 100 ppm sodium alginate; and (d) 1% (v/v) soybean oil and 100
408 ppm bovine serum albumin. (Normalized flux values are the quotient of the flux and the initial
409 flux readings).



410
 411 **Figure 7.** Water flux of PK-TFC, rPK-1-TFC, and rPK-2-TFC with the comprehensive fouling
 412 solution (containing (1% (v/v) soybean oil and 100 ppm each of bovine serum albumin, sodium
 413 alginate, and humic acid) over two 8 h cycle operations.

414 **4. Conclusion**

415 TFC membranes with reduced polyketone substrates were prepared using a facile method in
416 this study. Due to the chemical modification process, the reduced PK substrates exhibited highly
417 hydrophilic and oleophobic properties. As an effect of the membrane surface chemistry and the
418 intrinsic highly porous structure of polyketone, the TFC membranes showed outstanding water
419 flux and fouling resistance against a variety of model foulants, in comparison with the control
420 polyketone membrane. The rPK TFC membranes also have shown highly satisfactory self-
421 cleaning ability, as evidenced by high flux recovery ratios after simple backwashing. This study
422 proves that a simple modification and preparation method of the substrate for the preparation of
423 TFC membranes can be used for effective treatment of problematic oily wastewater.

424

425 **References**

- 426 [1] K. Lutchmiah, A.R.D. Verliefde, K. Roest, L.C. Rietveld, E.R. Cornelissen, Forward osmosis for application
427 in wastewater treatment: A review, *Water Research*, 58 (2014) 179-197.
- 428 [2] J.E. Kim, S. Phuntsho, F. Lotfi, H.K. Shon, Investigation of pilot-scale 8040 FO membrane module under
429 different operating conditions for brackish water desalination, *Desalination and Water Treatment*, 53
430 (2015) 2782-2791.
- 431 [3] F. Volpin, L. Chekli, S. Phuntsho, J. Cho, N. Ghaffour, J.S. Vrouwenvelder, H. Kyong Shon, Simultaneous
432 phosphorous and nitrogen recovery from source-separated urine: A novel application for fertiliser drawn
433 forward osmosis, *Chemosphere*, 203 (2018) 482-489.
- 434 [4] D.I. Kim, G. Gwak, M. Zhan, S. Hong, Sustainable dewatering of grapefruit juice through forward
435 osmosis: Improving membrane performance, fouling control, and product quality, *Journal of Membrane
436 Science*, 578 (2019) 53-60.
- 437 [5] R.R. Gonzales, M.J. Park, T.-H. Bae, Y. Yang, A. Abdel-Wahab, S. Phuntsho, H.K. Shon, Melamine-based
438 covalent organic framework-incorporated thin film nanocomposite membrane for enhanced osmotic
439 power generation, *Desalination*, 459 (2019) 10-19.
- 440 [6] F. Volpin, R.R. Gonzales, S. Lim, N. Pathak, S. Phuntsho, H.K. Shon, GreenPRO: A novel fertiliser-driven
441 osmotic power generation process for fertigation, *Desalination*, 447 (2018) 158-166.
- 442 [7] W.J. Lee, P.S. Goh, W.J. Lau, C.S. Ong, A.F. Ismail, Antifouling zwitterion embedded forward osmosis
443 thin film composite membrane for highly concentrated oily wastewater treatment, *Separation and
444 Purification Technology*, 214 (2018) 40-50.
- 445 [8] D.I. Kim, R.R. Gonzales, P. Dorji, G. Gwak, S. Phuntsho, S. Hong, H. Shon, Efficient recovery of nitrate
446 from municipal wastewater via MCDI using anion-exchange polymer coated electrode embedded with
447 nitrate selective resin, *Desalination*, 484 (2020) 114425.

448 [9] X. Wu, M. Shaibani, S.J.D. Smith, K. Konstas, M.R. Hill, H. Wang, K. Zhang, Z. Xie, Microporous carbon
449 from fullerene impregnated porous aromatic frameworks for improving the desalination performance of
450 thin film composite forward osmosis membranes, *Journal of Materials Chemistry A*, 6 (2018) 11327-11336.
451 [10] R.R. Gonzales, Y. Yang, M.J. Park, T.-H. Bae, A. Abdel-Wahab, S. Phuntsho, H.K. Shon, Enhanced water
452 permeability and osmotic power generation with sulfonate-functionalized porous polymer-incorporated
453 thin film nanocomposite membranes, *Desalination*, 496 (2020) 114756-114765.
454 [11] M.J. Park, R.R. Gonzales, A. Abdel-Wahab, S. Phuntsho, H.K. Shon, Hydrophilic polyvinyl alcohol
455 coating on hydrophobic electrospun nanofiber membrane for high performance thin film composite
456 forward osmosis membrane, *Desalination*, 426 (2018) 50-59.
457 [12] Y. Wang, Z. Fang, C. Xie, S. Zhao, D. Ng, Z. Xie, Dopamine incorporated forward osmosis membranes
458 with high structural stability and chlorine resistance, *Processes*, 6 (2018) 151.
459 [13] R.R. Gonzales, M.J. Park, L. Tijning, D.S. Han, S. Phuntsho, H.K. Shon, Modification of nanofiber support
460 layer for thin film composite forward osmosis membranes via layer-by-layer polyelectrolyte deposition,
461 *Membranes*, 8 (2018) 70-84.
462 [14] Y. Li, S. Qi, Y. Wang, L. Setiawan, R. Wang, Modification of thin film composite hollow fiber
463 membranes for osmotic energy generation with low organic fouling tendency, *Desalination*, 424 (2017)
464 131-139.
465 [15] J. Wang, S. Zhang, P. Wu, W. Shi, Z. Wang, Y. Hu, In situ surface modification of thin-film composite
466 polyamide membrane with zwitterions for enhanced chlorine resistance and transport properties, *ACS*
467 *Applied Materials & Interfaces*, 11 (2019) 12043-12052.
468 [16] H.M. Hegab, A. ElMekawy, T.G. Barclay, A. Michelmor, L. Zou, C.P. Saint, M. Ginic-Markovic, Fine-
469 tuning the surface of forward osmosis membranes via grafting graphene oxide: Performance patterns and
470 biofouling propensity, *ACS Applied Materials & Interfaces*, 7 (2015) 18004-18016.
471 [17] S. Jafarinejad, H. Park, H. Mayton, S.L. Walker, S.C. Jiang, Concentrating ammonium in wastewater by
472 forward osmosis using a surface modified nanofiltration membrane, *Environmental Science: Water*
473 *Research & Technology*, 5 (2019) 246-255.
474 [18] L. Cheng, A.R. Shaikh, L.-F. Fang, S. Jeon, C.-J. Liu, L. Zhang, H.-C. Wu, D.-M. Wang, H. Matsuyama,
475 Fouling-resistant and self-cleaning aliphatic polyketone membrane for sustainable oil-water emulsion
476 separation, *ACS Applied Materials & Interfaces*, 10 (2018) 44880-44889.
477 [19] Y. Sun, L. Cheng, T. Shintani, Y. Tanaka, T. Takahashi, T. Itai, S. Wang, L. Fang, H. Matsuyama,
478 Development of high-flux and robust reinforced aliphatic polyketone thin-film composite membranes for
479 osmotic power generation: Role of reinforcing materials, *Industrial & Engineering Chemistry Research*, 57
480 (2018) 13528-13538.
481 [20] K. Nakagawa, K. Uchida, J.L.C. Wu, T. Shintani, T. Yoshioka, Y. Sasaki, L.-F. Fang, E. Kamio, H.K. Shon,
482 H. Matsuyama, Fabrication of porous polyketone forward osmosis membranes modified with aromatic
483 compounds: Improved pressure resistance and low structural parameter, *Separation and Purification*
484 *Technology*, 251 (2020) 117400.
485 [21] L. Zhang, Y. Lin, L. Cheng, Z. Yang, H. Matsuyama, A comprehensively fouling- and solvent-resistant
486 aliphatic polyketone membrane for high-flux filtration of difficult oil-in-water micro- and nanoemulsions,
487 *Journal of Membrane Science*, 582 (2019) 48-58.
488 [22] L. Zhang, Y. Lin, H. Wu, L. Cheng, Y. Sun, T. Yasui, Z. Yang, S. Wang, T. Yoshioka, H. Matsuyama, An
489 ultrathin in situ silicification layer developed by an electrostatic attraction force strategy for ultrahigh-
490 performance oil-water emulsion separation, *Journal of Materials Chemistry A*, 7 (2019) 24569-24582.
491 [23] O. Ohsawa, K.-H. Lee, B.-S. Kim, S. Lee, I.-S. Kim, Preparation and characterization of polyketone (PK)
492 fibrous membrane via electrospinning, *Polymer*, 51 (2010) 2007-2012.
493 [24] Q. Zhang, Z. Zhang, L. Dai, H. Wang, S. Li, S. Zhang, Novel insights into the interplay between support
494 and active layer in the thin film composite polyamide membranes, *Journal of Membrane Science*, 537
495 (2017) 372-383.

- 496 [25] S. Wang, K. Gu, J. Wang, Y. Zhou, C. Gao, Enhanced the swelling resistance of polyamide membranes
497 with reinforced concrete structure, *Journal of Membrane Science*, 575 (2019) 191-199.
- 498 [26] I.L. Alsvik, M.-B. Hägg, Preparation of thin film composite membranes with polyamide film on
499 hydrophilic supports, *Journal of Membrane Science*, 428 (2013) 225-231.
- 500 [27] G.T. Gray, J.R. McCutcheon, M. Elimelech, Internal concentration polarization in forward osmosis:
501 Role of membrane orientation, *Desalination*, 197 (2006) 1-8.
- 502 [28] Y.-F. Guan, B.-C. Huang, Y.-J. Wang, B. Gong, X. Lu, H.-Q. Yu, Modification of forward osmosis
503 membrane with naturally-available humic acid: Towards simultaneously improved filtration performance
504 and antifouling properties, *Environment International*, 131 (2019) 105045.
- 505 [29] Y. Liu, B. Mi, Combined fouling of forward osmosis membranes: Synergistic foulant interaction and
506 direct observation of fouling layer formation, *Journal of Membrane Science*, 407-408 (2012) 136-144.

507